Binding of Antitumor Ruthenium Complexes to DNA and Proteins: A Theoretical Approach

Neva Bešker, Cecilia Coletti, Alessandro Marrone, and Nazzareno Re*

Dipartimento di Scienze del Farmaco, Università degli Studi G. d'Annunzio, Via Dei Vestini, 31, I-66100 Chieti, Italy

Received: March 19, 2007; In Final Form: June 15, 2007

The thermodynamics of the binding of the antitumor ammine, amine, and immine complexes of ruthenium(II) and ruthenium(III) to DNA and peptides was studied computationally using model molecules. We performed density functional calculations on several monofunctional ruthenium complexes of the formula $[Ru(NH_3)_5B]^{z+}$, where B is an adenine, guanine, or cytosine nucleobase or an 4-methylimidazole, a dimethylthioether, or a dimethylphosphate anion and $z = 2$ and 3. The pentammineruthenium fragment has been intensively studied and also constitutes a good model for a wide class of antitumor ammine, amine, and imine complexes of Ru(II) and Ru(III), while the considered bases/ligands have been chosen as models for the main binding sites of DNA, nucleobases, and phosphate backbone and proteins, histidyl, and sulfur-containing residue such as methionine or cysteine. Bond dissociation enthalpies and free energies have been calculated for all the considered metal binding sites both in the gas phase and in solution and allow building a binding affinity order for the considered nucleic acid or protein binding sites. The binding of guanine to some bifunctional complexes, $[Ru(NH_3)_4Cl_2]$, $[cis\text{-}RuCl_2(bpy)_2]$, and $[cis\text{-}RuCl_2(azpy)_2]$, has also been considered to evaluate the effect of a second labile chloro or aquo ligand and more realistic polypyridyl and arylazopyridine ligands.

1. Introduction

In attempts to find a new, metal-based anticancer drug with activity complementary to cisplatin, several ruthenium complexes have recently been investigated for their antitumor activity.[1−4] Many ruthenium compounds with nitrogen ligands, in particular ammine, amine, and aromatic imine Ru(II) and Ru(III) complexes, have been shown to exhibit good antitumor activity in screening studies and preferentially localize in tumor tissues. They vary from simple multichloro ammine compounds, such as $[cis\text{-}Ru(III)Cl_2(NH_3)_4]^+$ and $[fac\text{-}Ru(III)Cl_3(NH_3)_3]$,[4] to more complex polypyridyl, such as $[cis\text{-}Ru(II)Cl_2(bpy)_2]$ and $[mer\text{-}Ru(III)Cl_3(terpy)]$,[5] heterocyclic, such as (HInd)$[trans\text{-}Ru(III)Cl_4(Ind)_2]$ (Ind = indazole) and (HIm)$[trans\text{-}Ru(III)Cl_4(Im)_2]$ (Im = imidazole),[1c,6−8] and arylazopyridine complexes, such as $[trans\text{-}Ru(II)Cl_2(azpy)_2]$ (azpy = 2-(phenylazo)pyridine).[9] Good antitumor activity has also been shown by DMSO complexes (DMSO = dimethyl sulfoxide), i.e., $[trans\text{-}Ru(II)Cl_2(DMSO)_4]$,[10] $Na[trans\text{-}Ru(III)Cl_4(Im)(DMSO)]$,[11] and (HIm)$[trans\text{-}Ru(III)Cl_4(Im)(DMSO)]$,[12] and organometallic arene complexes, i.e., $(\eta^6\text{-benzene})Ru(II)(DMSO)Cl_2$[13] and $[(\eta^6\text{-arene})Ru(II)(en)Cl]^+$.[14] Moreover, some ruthenium complexes have recently been shown to display interesting antimetastatic properties, and two of them, notably (HIm)-$[trans\text{-}Ru(III)Cl_4(Im)(DMSO)]$ (NAMI-A)[12] and (HInd)$[trans\text{-}Ru(III)Cl_4(Ind)_2]$ (KP1019),[6,8] have completed phase I clinical trials.

Despite the plethora of biological investigations both in vitro and in vivo, the mode of action of these compounds at a molecular level is largely not understood and of much interest.[1−4] Therefore, a good understanding of the interaction of ruthenium complexes with models of binding sites present in DNA is of paramount importance to unravel the mode of action of ruthenium-based drugs.

It is known that Ru(II) and Ru(III) complexes tend to selectively bind to imine sites in biomolecules, which are not protonated at neutral pH, thereby leaving their lone pair available for metal ion coordination. As a consequence, ruthenium complexes are expected to coordinate histidyl imidazole nitrogens on proteins and the nitrogen sites of purine nucleotides, thus targeting in vivo proteins and nucleic acids.[1]

On the basis of the relative pK_a, ruthenium binding to the surface-accessible histidyl imidazoles of proteins is expected to be stronger than to DNA nucleobases[15] and, indeed, has been observed in several blood proteins, such as albumin and transferrin. [16] In particular, binding to transferrin is believed to facilitate ruthenium transport into cells.[17] Ruthenium binding to sulfur (S donor/thiolate) compounds has also been observed, but the resulting complexes are often kinetically unstable, especially in the presence of oxygen.[18]

However, there is increasing evidence in the literature that the antitumor properties of many of these ruthenium complexes are due to their interactions with DNA nucleobases.[2b,5b,19] Among the various coordinating sites available on a polynucleotide, much experimental evidence indicates that the preferred binding target of Ru(II) and Ru(III) is the N7 site of guanine, although binding to adenine and cytosine may also occur.[2b,5b,15,19]

The significant structural differences between ruthenium and most platinum-based antitumor drugs give a promise that ruthenium-based drugs could be suitable alternatives to cisplatin and carboplatin. Ruthenium is a group VIII metal which occurs in aqueous solution predominantly as Ru(II) and Ru(III) and in both oxidation states is invariably six-coordinated with octahedral geometry.[20] Due to the octahedral structure of Ru(II) and Ru(III) complexes as opposed to the square-planar geometry of Pt(II), ruthenium complexes could act in a different way from that of cisplatin, which is known to bend DNA by cross-linking adjacent guanine bases.[21] Intra- or interstrand DNA cross-linking

* To whom correspondence should be addressed. E-mail: nre@unich.it.

10.1021/jp072182q CCC: $37.00
Published on Web 08/02/2007

SCHEME 1: Aquation Reaction of the Dichloro Ruthenium(II) Complexes

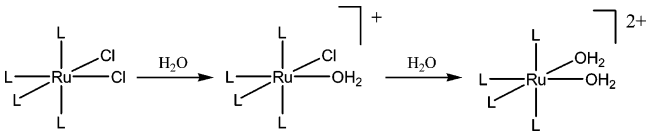

has been observed also for some antitumor ruthenium complexes,[5a,22,23] such as, for instance, [*cis*-Ru(III)$Cl_2(NH_3)_4$]$^+$, [*cis*-Ru(II)Cl_2(bpy)$_2$],[5a] (HIm)-[*trans*-Ru(III)Cl_4(Im)(DMSO)], and (HInd)[*trans*-Ru(III)Cl_4(Ind)$_2$].[23] These complexes lose their chloride ligands and transform into the more reactive aquated species which then undergoes water substitution by one or two DNA nucleobases,[1−4] Scheme 1. Other complexes, such as (HInd)[*trans*-Ru(III)Cl_4(Ind)$_2$], have been show to cross-link DNA and topoisomerase II, the enzyme controlling the topological properties of DNA, and help maintain the structural organization of the mitotic chromosomal scaffold in the replication, transcription, recombination, and segregation of chromosomal pairs during cell division.[24] It is therefore not surprising that multichloro or multiaquo complexes exhibit the best antitumoral activity, although also monochloro or monoaquo compounds are active.[1−4]

Another important difference between platinum and ruthenium complexes consists in the range of oxidation states (Ru^{II}, Ru^{III}, and Ru^{IV}) accessible under physiological conditions for ruthenium, which allows the so-called "activation by reduction" mechanism.[4,25] Inside tumor cells pH and O_2 contents are lower than in surrounding normal tissue,[26] and as a consequence, the electrochemical potential inside solid tumors is also lower.[27] This favors the presence of Ru(II) relative to Ru(III), and it is believed that Ru(III) complexes may serve as prodrugs that are activated by reduction in vivo to coordinate more rapidly to biomolecules. Indeed, the lower charge of Ru(II) would make its complexes more labile than those of Ru(III).[28] Reducing agents like glutathione in the cell and ascorbic acid in the blood may also lead to reduction of ruthenium(III) complexes.[29]

Following these studies there has been considerable interest in the interaction of Ru(II) and Ru(III) complexes with nucleobases, nucleotides, or DNA fragments.[30] In particular, to elucidate ruthenium binding sites in DNA, several complexes between ruthenium and N9-alkylated purines and N1-alkylated pyrimidines, nucleosides, and nucleotides have been synthesized and studied by NMR and X-ray diffraction.[30−31]

Although interactions between ruthenium and nucleobases have been the subject of intense experimental research, to the best of our knowledge no general quantum mechanical study has been performed on the ruthenium complexes of purine and pyrimidine nucleobases. Only a few calculations have been performed either at the semiempirical level[32] or on a specific ruthenium complex.[33]

In this work we investigated the electronic structure of several monofunctional ruthenium complexes of the formula [Ru$(NH_3)_5$B]$^{z+}$, where B is an adenine, guanine, or cytosine nucleobase and a 4-methylimidazole (hereafter indicated as MeIm), a dimethylthioether, or a dimethylphosphate anion, and $z = 2$ and 3 (Chart 1). The considered pentaammineruthenium fragment has been intensively studied and constitutes also a good model for a wide class of antitumor ammine, amine, and imine complexes of Ru(II) and Ru(III), while the considered bases have been chosen as models for the main binding sites of DNA, nucleobases and phosphate backbone, and proteins, histidyl, and sulfur-containing residue such as methionine or cysteine. Thymine was not considered since it has not been observed to bind ruthenium complexes, consistent with the lack of a sufficiently strong binding site. Full geometry optimizations and density functional calculations were performed for all possible coordination modes between the [Ru$(NH_3)_5$]$^{z+}$ fragment and each base B. Bond dissociation enthalpies and free energies have been calculated for all the considered Ru−B bonds both in the gas phase and in solution and allow us to build a binding affinity order for the considered nucleic acid or protein binding sites. We also considered the binding of a guanine molecule—the most tightly bound nucleobase—to some bifunctional complexes, i.e., [Ru$(NH_3)_4Cl_2$] and [Ru$(NH_3)_4(H_2O)_2$]$^{2+}$, to evaluate the effect of a second labile (chloro or aquo) coordination site and [*cis*-Ru(II)Cl_2(bpy)$_2$] and [*cis*-Ru(II)Cl_2(azpy)$_2$] to consider more realistic polypyridyl and arylazopyridine ligands.

CHART 1: Considered Bases[a]

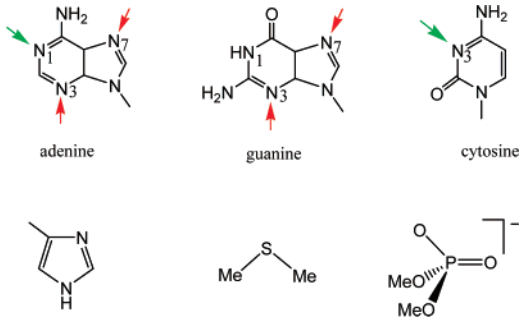

[a] For the nucleobases arrows indicate coordination sites, either those available for binding in DNA (red arrows) or those involved in base pairing (green arrows).

2. Computational and Methodological Details

The calculations reported in this paper are based on the ADF (Amsterdam Density Functional) program package described elsewhere.[34] Its main characteristics are the use of a density fitting procedure to obtain accurate Coulomb and exchange potentials in each SCF cycle, the accurate and efficient numerical integration of the effective one-electron Hamiltonian matrix elements, and the possibility to freeze core orbitals.

The molecular orbitals were expanded in an uncontracted triple-ζ Slater-type orbitals (STO) basis set for all main-group atoms. For ruthenium orbitals we used a double-ζ STO basis set for 3s and 3p and a triple-ζ STO basis set for 3d and 4s. As polarization functions we used one 4p function for ruthenium, one 3d for C, N, and O, and one 2p for H. The inner shell cores (1s-2/3p for Ru, 1s for C, N, and O) have been kept frozen.

The LDA exchange correlation potential and energy were used together with the Vosko−Wilk−Nusair parametrization[35] for homogeneous electron gas correlation, including the Becke's nonlocal correction[36] to the local exchange expression and the Perdew's nonlocal correction[37] to the local expression of correlation energy. Molecular structures of all considered complexes were optimized at this gradient-corrected level without any symmetry constraint. Since relativistic effects play an important role in describing the electronic structure and relative energetics of the species containing a second-row transition metal, such as ruthenium, they were taken into account by the Pauli formalism, the Pauli Hamiltonian including first-order scalar relativistic corrections (Darwin and mass velocity) while neglecting spin−orbit corrections.[38] Restricted calculations were performed on the closed shell singlet state of the Ru(II) complexes, while unrestricted calculations were carried out on the doublet state of the Ru(III) open shell systems, in agreement with the known magnetic behavior of the $d^6(t_{2g}^6)$ and $d^5(t_{2g}^5)$

TABLE 1: Main Geometrical Parameters Calculated for $[Ru(NH_3)_5B]^{z+}$ Complexes

B	Ru−XB	Ru−N_1	Ru−N_2	Ru−N_3	Ru−N_4	Ru−N_{trans}	H_2NH−O	H_2NH−N
(a) $[Ru(NH_3)_5B]^{2+}$ complexes (bond distances in Å)								
NH_3	2.178	2.178	2.178	2.178	2.178	2.178		
Me_2S	2.333	2.175	2.175	2.180	2.180	2.234		
A1	2.146	2.179	2.195	2.180	2.166	2.196		2.035
A3	2.121	2.186	2.186	2.170	2.168	2.208		
A7	2.120	2.154	2.169	2.183	2.163	2.185		1.898
C	2.189	2.153	2.163	2.214	2.199	2.186	1.819	
G3	2.170	2.196	2.198	2.156	2.155	2.188		
G7	2.096	2.153	2.165	2.180	2.175	2.188	1.773	
MeIm	2.116	2.165	2.165	2.178	2.174	2.201		
$Me_2PO_4^-$	2.152	2.151	2.154	2.167	2.163	2.152	1.867	
(b) $[Ru(NH_3)_5B]^{3+}$ complexes (bond distances in Å)								
NH_3	2.178	2.178	2.178	2.178	2.178	2.178		
Me_2S	2.290	2.178	2.180	2.193	2.193	2.206		
A1	2.111	2.181	2.192	2.181	2.170	2.203		2.049
A3	2.076	2.182	2.179	2.180	2.180	2.199		
A7	2.097	2.154	2.166	2.197	2.171	2.193		1.920
C	2.130	2.141	2.159	2.208	2.193	2.184	1.792	
G3	2.136	2.197	2.199	2.165	2.160	2.186		
G7	2.088	2.150	2.162	2.196	2.186	2.188	1.800	
MeIm	2.078	2.161	2.163	2.190	2.187	2.202		
$Me_2PO_4^-$	1.986	2.154	2.152	2.169	2.165	2.179	1.832	

octahedral ruthenium complexes with medium to strong field ligands in these oxidation states.

Vibrational frequency calculations were performed employing the same gradient-corrected exchange-correlation functional and a reduced basis set of double-ζ plus polarization quality (triple-ζ for the metal) to derive the zero-point energy (ZPE) and vibrational energy corrections at room temperature. To evaluate solvent effects, solvation free energies were estimated by a single-point calculation using the conductor-like screening model COSMO[39] on the optimized gas-phase geometries. A dielectric constant of 78.2 was used to represent the water solvent. The radii used for the atoms (Å) were as follows: H, 1.29; C, 2.00; N, 1.83; O, 1.71; Ru, 2.30. ZPE corrections, thermal corrections to the enthalpy, entropy terms, and solvation free energies have been employed to calculate Gibbs free energies for the Ru−B bond formation at 298 K both in the gas phase, $\Delta G°$(gas), and in solution, $\Delta G°$(sol). We also evaluated the gas-phase bond formation electronic energies, D_e, enthalpies, $\Delta H°$(gas), and an approximate estimate of the bond formation enthalpies in solution as $\Delta H°(\text{sol}) = \Delta H°(\text{gas}) + \Delta\Delta G_{solv}$, including the solvation entropy contributions that cannot be separated from $\Delta\Delta G_{solv}$.

Proton affinities of the considered bases, including all protonation sites of nucleobases, have been calculated as the gas-phase enthalpies at 298 K of the deprotonation reaction

$$BH^+ \rightarrow B + H^+$$

The corresponding pK_a's have been calculated as

$$pK_a = \Delta G°_{deprot}(\text{sol})/2.303\,RT$$

where $\Delta G°_{deprot}$(sol) is the Gibbs free energy at 298 K for the deprotonation reaction, calculated as described above for the Ru−B bond formation, R is the gas constant, and T is the temperature.

In order to separate the contributions from σ donation and π back-donation we employed an analysis of the Ru(II)−B bond dissociation energies based on the extended transition-state method.[40a] The bond dissociation energy is decomposed into a number of contributions

$$\Delta E(\text{Ru−B}) = -[\Delta E_{str} + \Delta E_{elst} + \Delta E_{Pauli} + \Delta E_{orb}]$$

The first term, ΔE_{str}, is the strain energy necessary to convert the fragments from their equilibrium geometries to the conformation they assume in the optimized structure of the overall complex and corresponds to the sum of the fragments strain energies, $E_{str}[Ru(NH_3)_5^{2+}] + E_{str}[B]$. ΔE_{elst} represents the electrostatic interaction of the nuclear charges and the unmodified electronic charge density of one fragment with those of the other fragment, while ΔE_{Pauli} is the four-electron destabilizing interactions between occupied orbitals (Pauli repulsion) and together correspond to the steric repulsion between the two fragments. ΔE_{orb}, known as the orbital interaction term, represents the attracting orbital interactions which give rise to the energy lowering upon coordination. This term may be broken up into contributions from the orbital interactions within the various irreducible representations Γ of the overall symmetry group of the system according to the decomposition scheme proposed by Ziegler.[40b] This decomposition scheme is particularly useful in the considered complexes as it allows one to separate the energy contributions corresponding to σ donation ($E_{a'}$) and π back-donation ($E_{a''}$). Indeed, the ligand to metal σ donation takes place into the a′ representation, while the metal to ligand π back-donation takes place into the a″ representation. Such an analysis is limited to closed shell systems and has been thus carried out for Ru(II) complexes only. To perform it, we first reoptimized all complexes in C_s symmetry: the main geometrical parameters and gas-phase bond dissociation energies show negligible deviations from the corresponding values obtained without any symmetry constraint, except for the G7, A1, and A7 complexes which may form a hydrogen bond between an equatorial ammonia ligand and a carbonyl or an ammine group on the nucleobase (see below).

3. Results and Discussion

3.1. Geometries. All $[Ru(NH_3)_5(B)]^{z+}$ complexes, including also an amino, chloro, and aquo ligand B, were fully optimized, and for the nucleobases, all possible coordination modes were considered. Indeed, when considering nucleobases, ruthenium may bind to the N7 and N3 atoms of guanine, the N7, N3, and N1 atoms of adenosine, and the N3 atom of cytosine, see Chart 1, although the N1 of adenine and the N3 of cytosine, being involved in base pairing, are expected to be less available for metal binding. Binding to the carbonyl oxygen atoms of guanine

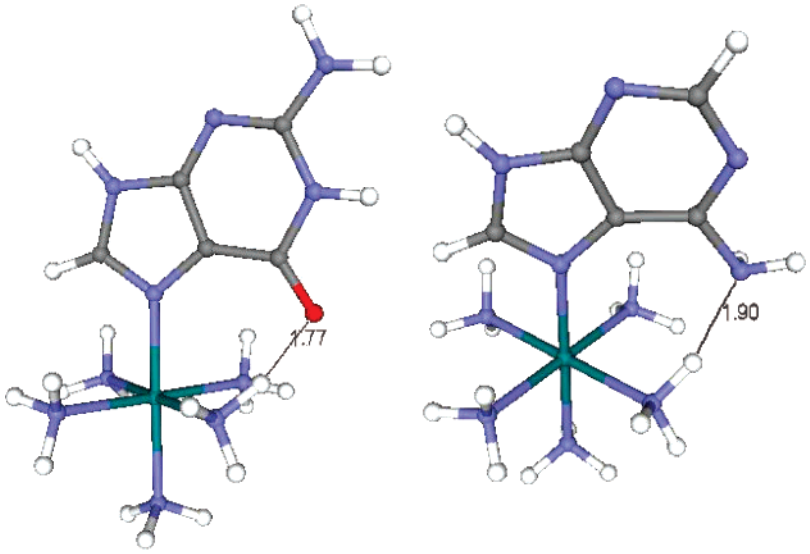

Figure 1. Geometries of the (a) $[Ru(II)(NH_3)_5(G7)]^{2+}$ and (b) $[Ru(II)(NH_3)_5(A7)]^{2+}$ complexes.

and cytosine was not considered since these atoms are strongly involved in base pairing in DNA. The main geometrical parameters calculated for these $[Ru(NH_3)_5(B)]^{z+}$ complexes are reported in Tables 1 and S1 (Supporting Information), and the geometries of the most representative N7-bound guanine and adenine complexes of Ru(II) are shown in Figure 1. All complexes have essentially octahedral coordination around the ruthenium atom, and for those with nucleobases and imidazole, the plane of the heterocyclic base lies perpendicular to the equatorial $Ru(NH_3)_4$ plane, almost bisecting the equatorial N−Ru−N angles to reduce steric hindrance with the equatorial ammines. The Ru−N(B) bond lengths are similar for all bases being slightly shorter in the Ru(III) than in the Ru(II) oxidation state, as expected on the basis of the higher positive charge, and falling in the range 2.10−2.19 Å for Ru(II) and 2.08−2.18 Å for Ru(III) complexes, see Table 1. The calculated structures show a hydrogen bond between one of the equatorial NH_3 ligands and the carbonyl group in guanine N7 and cytosine N3 complexes which is probably responsible for the stronger bond energies calculated for these two nucleobases, see below. The presence of the hydrogen bond is indicated by (i) the short C═O−H−N contacts (1.77/1.78 and 1.79/1.82 Å, respectively, for the guanine and cytosine complexes of Ru(II)/Ru(III)), (ii) the deviation from the octahedral 90° value of the H_3N−Ru−N(B) angle (86°/86° and 87°/86°, respectively, for the guanine and cytosine complexes of Ru(II)/Ru(III)), and (iii) the elongation of the involved N−H ammine bond by about 0.005 Å compared to the remaining two N−H ammine bonds. A similar hydrogen bond is also observed between an equatorial NH_3 ligand and the NH_2 group in the adenine N1 and N7 complexes, although apparently weaker as shown by the longer −N−H−N contacts of 1.90−2.05 Å. These hydrogen bonds are very similar to those observed for the corresponding guanine and adenine adducts of cisplatin.[21] For instance, DFT calculations at a similar level of theory[41] have shown C═O−H−N contact distances of 1.74 and 2.10 Å, respectively, for the guanine and adenine *cis*-$[PtCl(NH_3)_2(B)]^+$ complexes. To validate our theoretical approach a comparison has been made between the theoretical and experimental structure of one member of this class of complexes. Since no X-ray structure is available for Ru(II) pentaammino nucleobase complexes, we considered 7-$[(Hyp)(NH_3)_5Ru(III)]^{3+}$, Hyp = hypoxantine, whose geometry has been compared with that

SCHEME 2: Thermodynamical Cycle Employed To Include Solvation Effects into the Ru−B Bond Dissociation Free Energy

$$\begin{array}{ccc} [Ru(NH_3)_5(B)]^{z+}(g) & \xrightarrow{\Delta G(g)} & [Ru(NH_3)_5]^{z+}(g) + B(g) \\ \downarrow \Delta G_{solv}([Ru(NH_3)_5(B)]^{z+}) & & \downarrow \Delta G_{solv}([Ru(NH_3)_5]^{z+}) \quad \downarrow \Delta G_{solv}(B) \\ [Ru(NH_3)_5(B)]^{z+}(aq) & \xrightarrow{\Delta G(aq)} & [Ru(NH_3)_5]^{z+}(aq) + B(aq) \end{array}$$

of 7-[(Hyp) $(NH_3)_5Ru]Cl_3 \cdot 3H_2O$.[30c] The calculated geometrical parameters are compared with the experimental X-ray data in Table 2 that shows a good agreement with bond distances within 0.05 Å and bond angles within 2°. Particulary striking is the agreement of the $Ru-N_B$ distance, within 0.001 Å, while the only significant discrepancy, by 0.1 Å, is observed for the Ru−NH_3 distance of the ammine trans to the hypoxantine base.

3.2. Bond Dissociation Energies. Ru−B bond dissociation energies have been calculated as the difference between the energy of the optimized complexes and those of the two relaxed $[Ru(NH_3)_5]^{z+}$ and B fragments. The solvation effect has been included through the COSMO approach according to Scheme 2. The calculated gas-phase and solution bond dissociation enthalpies and free energies are reported in Tables 3 and 4, respectively, for Ru(II) and Ru(III) together with the solvation energies for the complex and the base and the overall solvation corrections. Solvation energies for the dicationic and tricationic ruthenium pentammine fragments follow the expected trend with

TABLE 2: Comparison between Calculated and Experimental Geometrical Parameters for 7-$[Ru(III)(NH_3)_5(Hyp)]^{3+}$

parameter	calculated	X-ray
Ru−N7	2.088	2.087(9)
Ru−N10	2.145	2.105(7)
Ru−N11	2.192	2.115(7)
Ru−N12	2.180	2.081(9)
N7−Ru−N10	93.8	92.3(2)
N7−Ru−N11	89.5	91.3(2)
N7−Ru−N12	177.8	179.1(8)
N10−Ru−N12	88.2	87.1(2)
N11−Ru−N12	89.5	89.3(2)

TABLE 3: Bond Dissociation Enthalpies and Free Energies (kJ mol^{-1}) in the Gas Phase and Solution for the Ru(II)−B Bonds in the Considered [Ru(NH$_3$)$_5$B]$^{2+}$ Complexes

B	D_e	ΔH^{298}(gas)	ΔG^{298}(gas)	ΔH^{298}(aq)	ΔG^{298}(aq)	$\Delta\Delta G_{solv}$[b]	G_{solv}(B)	G_{solv}[a]
NH_3	168	159	113	93	46	−67	−14	−767
Cl^-	923	918	884	45	11	−874	−314	−260
H_2O	109	102	56	35	−11	−67	−21	−774
Me_2S	191	191	125	100	35	−91	−8.4	−737
A1	202	200	131	64	−4.3	−136	−56	−740
A3	207	198	141	79	22	−119	−56	−757
A7	190	180	122	51	−7.7	−129	−56	−747
C	261	250	188	70	8.8	−180	−75	−716
G3	109	103	41	11	−51	−92	−93	−821
G7	326	317	256	105	45	−211	−93	−701
MeIm	237	226	173	84	31	−143	−37	−714
$Me_2PO_4^-$	906	902	834	52	−16	−850	−272	−243

[a] Solvation energy of the considered [Ru(NH$_3$)$_5$B]$^{2+}$ complex. [b] $\Delta\Delta G_{solv} = G_{solv}([Ru(NH_3)_5]^{2+}) + G_{solv}(B) - G_{solv}([Ru(NH_3)_5B]^{2+})$ with $G_{solv}(Ru(NH_3)_5^{2+}) = -820$ kJ/mol.

TABLE 4: Bond Dissociation Enthalpies and Free Energies Values (kJ mol^{-1}) in the Gas Phase and Solution for the Ru(III)−B Bonds in the Considered [Ru(NH$_3$)$_5$B]$^{3+}$ Complexes

B	D_e	ΔH^{298}(g)	ΔG^{298}(g)	ΔH^{298}(aq)	ΔG^{298}(aq)	$\Delta\Delta G_{solv}$[b]	G_{solv}(B)	G_{solv}[a]
NH_3	258	242	205	110	73	−132	−14	−1719
Cl^-	1464	1456	1428	122	94	−1334	−314	−817
H_2O	189	177	133	48	3	−130	−21	−1729
Me_2S	343	335	282	85	32	−250	−8.4	−1596
A1	423	414	353	76	15	−338	−56	−1555
A3	454	440	391	88	39	−352	−56	−1541
A7	398	386	332	60	6	−326	−56	−1567
C	462	443	392	81	30	−362	−75	−1551
G3	234	313	252	8	−53	−305	−93	−1625
G7	595	582	519	131	68	−450	−93	−1480
MeIm	428	414	361	105	52	−309	−37	−1565
$Me_2PO_4^-$	1501	1487	1434	124	71	−747	−272	−1362

[a] Solvation energy of the considered [Ru(NH$_3$)$_5$B]$^{3+}$ complex. [b] $\Delta\Delta G_{solv} = G_{solv}([Ru(NH_3)_5]^{3+}) + G_{solv}(B) - G_{solv}([Ru(NH_3)_5B]^{3+})$ with $G_{solv}(Ru(NH_3)_5^{3+}) = -1837$ kJ/mol.

SCHEME 3: Thermodynamical Cycle Employed To Include Solvation Effects into the Reaction Free Energy for Substitution of the Aquo Ligand by the Base B in [Ru(NH$_3$)$_5$(H$_2$O)]$^{z+}$

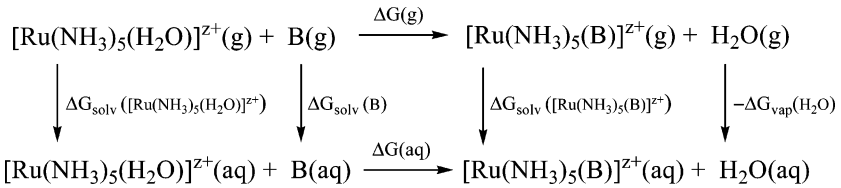

values of −820 and −1837 kJ mol^{-1} calculated, respectively, for [Ru(NH$_3$)$_5$]$^{2+}$ and [Ru(NH$_3$)$_5$]$^{3+}$. Lower solvation energies have been calculated for both the neutral (in the range from −8 to −93 kJ mol^{-1}) and the anionic (from −272 to −314 kJ mol^{-1}) bases.

The large bond dissociation enthalpies and free energies calculated in the gas phase, 40−320 kJ mol^{-1} for neutral and ca. 900 kJ mol^{-1} for anionic bases for Ru(II) and 130−580 kJ mol^{-1} for neutral and ca. 1500 kJ mol^{-1} for anionic bases for Ru(III), are due to the strong electrostatic attraction of the positively charged metal fragments with the negatively charged or polar base. These values are considerably reduced in aqueous solution, mainly due to the high solvation energies of the charged metal fragments, and the bond dissociation free energies assume values below 45 kJ mol^{-1} for Ru(II) and 68 kJ mol^{-1} for Ru(III) with some of the complexes even unstable toward dissociation (A(N1), A(N7), G(N3), and (MeO)$_2$PO$_2^-$ for Ru(II) and G(N3) for Ru(III)). The decrease is larger for the anionic dimethylphosphate base due to its high solvation energy and, to a lesser extent, for guanine and cytosine, the nucleobases with the highest solvation energies. Moreover, while the gas-phase bond dissociation free energies are much higher for the more charged Ru(III) fragments than for Ru(II), with a difference of ca. 200−600 kJ mol^{-1}, the values in solution are quite similar due to the larger solvation energy of the Ru(III) fragment.

The bond dissociation free energies reported in Tables 3 and 4 indicate that in aqueous solution guanine, coordinated at N7, is the most strongly bound base for Ru(II) and, within 3 kJ mol^{-1}, also for Ru(III), in agreement with experimental evidence indicating that guanine N7 is the preferred site for ruthenium binding. More in detail, for Ru(II), the calculated binding order is (MeO) $_2$PO$_2^-$ > G(N7) > C(N3) > MeIm > A(N3) > A(N1) > Me$_2$S > A(N7) > G(N3) in gas phase, while it is G(N7) > Me$_2$S > MeIm > A(N3) > C(N3) > A(N7) > A(N1) > (MeO)$_2$PO$_2^-$ > G(N3) in solution with a strong decrease of the dimethylphosphate binding order going from the gas phase to solution due to the high solvation energy of this anionic species and to a lesser extent also of the cytosine order and an increase of the Me$_2$S order due to its low solvation energy. These results suggest that although the guanine N7 is the preferred site for ruthenium(II) binding, also the imidazole-containing histidyl residue or the sulfur-containing methionine and cysteine residues in proteins are favorable binding sites with binding free energies only 10−14 kJ mol^{-1} lower. It is also important to note that while the gas-phase binding free energy of the dimethylphosphate anion to Ru(II) is higher than those of all

the other neutral bases, as expected on the basis of electrostatic considerations, the bond dissociation free energy in solution is much lower, with a negative value, suggesting that binding of Ru(II) complexes to the anionic phosphate groups of the DNA backbone is not a favored process. Table 3 also shows that complexation at N3 of adenine or N3 of cytosine is relatively favorable, but since these sites are involved in hydrogen bonding in duplex DNA, they are not available for binding to ruthenium in vivo.

The calculated binding order for Ru(III) is $(MeO)_2PO_2^-$ > G(N7) > C(N3) > A(N3) > MeIm > A(N1) > A(N7) > Me_2S > G(N3) in the gas phase, while it is $(MeO)_2PO_2^-$ > G(N7) > MeIm > A(N3) > Me_2S > C(N3) > A(N1) > A(N7) > G(N3) in solution with minor bonding order changes, with respect to Ru(II), going from the gas phase to solution. In particular, in spite of the strong decrease of the dimethylphosphate bond free energy passing from the gas phase to solution, the Ru(III)−phosphate is still the strongest bond in aqueous solution, probably because of the stronger electrostatic interaction between the anionic phosphate and the tricationic Ru(III) fragment. This result is very different from that obtained for the Ru(II)−phosphate bond, which is calculated to be unstable in solution, and suggests that the Ru(III) complexes in vivo could bind strongly to the phosphate anionic groups of the DNA backbone or also to other anionic groups on the proteins surfaces. Interestingly, this result is consistent with the experimentally observed low antitumor activity of the unreduced Ru(III) species and supports the activation by reduction mechanism. The bond dissociation free energy in solution for guanine N7 is only 3 kJ mol^{-1} lower than that for dimethylphosphate, while that for imidazole is 19 kJ mol^{-1} and that for the soft Me_2S base is 39 kJ mol^{-1} lower, suggesting that imidazole-containing histidyl residue or the sulfur-containing methionine and cysteine residues in proteins are less favorable binding sites for the hard Ru(III) species.

The Ru(II) bond dissociation enthalpies and free energies of guanine and adenine are comparable to the corresponding values calculated for the binding of these two bases to cisplatin in previous computational studies.[41−43] For instance, at the B3LYP/ccVTZ//B3LYP/6-31G** level of theory, for $[Pt(NH_3)_2Cl(B)]^+$ the bond dissociation enthalpies in the gas phase are 337 and 265 kJ mol^{-1} and the bond dissociation free energies in solution are 67 and 48 kJ mol^{-1}, respectively, for guanine and adenine, while for $[Pt(NH_3)_2(H_2O)(B)]^{2+}$ the corresponding values are 509 and 400 kJ mol^{-1} in the gas phase and 59 and 14 kJ mol^{-1} in solution.[41]

Tables 3 and 4 also report the bond dissociation enthalpies and free energies for the Ru−ammino, −chloro, and −aquo bonds. They show similar trends to those observed for the other Ru−B bonds, and the free energy values in solution are very small for the Ru−aquo bond—even negative for Ru(II)—and very large for the Ru−ammino bond, consistent with the experimental evidence that aquo complexes most easily undergo substitution while Ru−ammino bonds are inert. Moreover, the Ru−chloro bond free energy is small for Ru(II) but large for Ru(III), reflecting the high inertness of Ru(III) complexes with anionic ligands, as already discussed above for dimethylphosphate.

We then explicitly studied the thermodynamics of the binding of the considered antitumor ruthenium complexes to the DNA and protein binding sites. As mentioned above, the most active antitumor Ru compounds are multichloro ammino, amino, and imino complexes which loose their chloride ligands, transforming into the corresponding aquated species which then more easily undergo substitution by the binding base. Within our monofunctional model the ruthenium complex actually reacting with the bases B is the pentaamminemonoaquo $[Ru(H_2O)(NH_3)_5]^{2+}$, according to the reaction

$$[Ru(NH_3)_5(H_2O)]^{z+} + B \rightarrow [Ru(NH_3)_5(B)]^{z+} + H_2O$$

for which we evaluated the reaction enthalpies and free energies.

TABLE 5: Reaction Enthalpies and Free Energies (kJ mol^{-1}) in the Gas Phase and Solution for the Water Substitution Reaction by the Bases B: $[Ru(NH_3)_5(H_2O)]^{2+} + B \rightarrow [Ru(NH_3)_5B]^{2+} + H_2O$

B	ΔH^{298}(gas)	ΔG^{298}(gas)	ΔH^{298}(aq)	ΔG^{298}(aq)
NH_3	−57	−61	−58	−57
Cl^-	−816	−832	−10	−22
Me_2S	−89	−73	−65	−46
A1	−98	−79	−29	−6.7
A3	−96	−89	−44	−33
A7	−78	−70	−16	−3.3
C	−148	−136	−35	−20
G3	−1.3	11	24	40
G7	−215	−204	−70	−56
MeIm	−124	−121	−49	−42
$Me_2PO_4^-$	−800	−778	−17	−4.2

TABLE 6: Reaction Enthalpies and Free Energies (kJ mol^{-1}) in the Gas Phase and Solution for the Water Substitution Reaction $[Ru(NH_3)_5H_2O]^{3+} + B \rightarrow [Ru(NH_3)_5B]^{3+} + H_2O$

B	ΔH^{298}(gas)	ΔG^{298}(gas)	ΔH^{298}(aq)	ΔG^{298}(aq)
NH_3	−65	−72	−62	−70
Cl^-	−1279	−1295	−74	−91
Me_2S	−158	−149	−37	−29
A1	−237	−220	−28	−12
A3	−263	−258	−40	−36
A7	−209	−199	−12	−3
C	−266	−259	−33	−27
G3	−136	−119	40	56
G7	−405	−386	−83	−65
MeIm	−237	−228	−57	−49
$Me_2PO_4^-$	−1310	−1301	−76	−68

The solvation effect has been included again through the PCM approach according to the reaction scheme reported in Scheme 3. The calculated reaction enthalpies and free energies in the gas phase and solution are reported in Tables 5 and 6, respectively, for Ru(II) and Ru(III). It is worth noting that the values in solution, upon sign change, also give a more accurate estimate of the corresponding Ru−B bond dissociation enthalpies and free energies in solution, accounting explicitly for the water molecule in the first solvation sphere of the metal fragment. Tables 5 and 6 show that the reaction free energies for substitution of the water molecule by all considered bases in both $[Ru(H_2O)(NH_3)_5]^{2+}$ and $[Ru(H_2O)(NH_3)_5]^{3+}$ complexes are negative, with the exception of G3, consistent with the experimentally observed easy substitution of water by these bases. Their values are in qualitative agreement, within 10 kJ mol^{-1}, with the bond dissociation enthalpies and free energies calculated without inclusion of an explicit water molecule (Tables 3 and 4) and show therefore exactly the same trends discussed above.

3.3. Bifunctional Complexes with Polypyridyl and Arylazopyridine Ligands. Since the most active among the ammine, amine, and imine ruthenium complexes are multichloro species, which may bind to two nucleobases in the duplex DNA structure, we performed analogous calculations on the binding of nucleobases to some bifunctional complexes, such as the

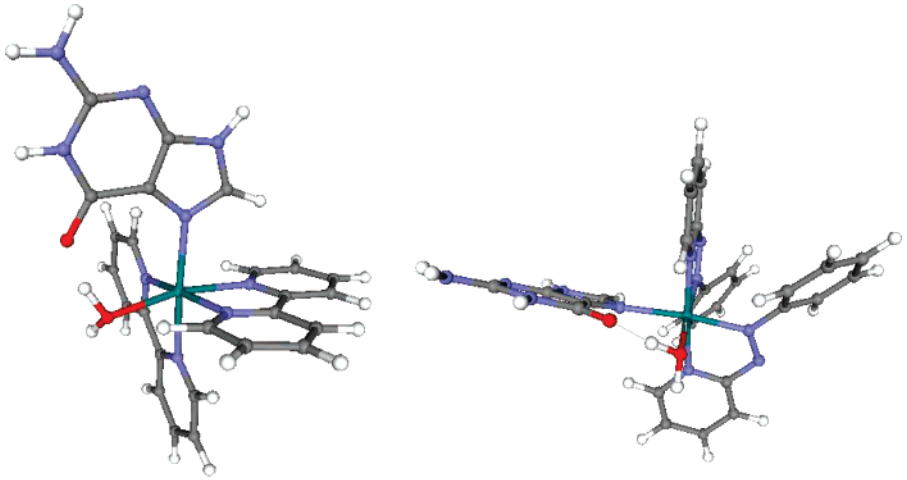

Figure 2. Geometries of the (a) $[Ru(II)(bpy)_2(H_2O)(G7)]^{2+}$ and (b) $[Ru(II)(azpy)_2(H_2O)(G7)]^{2+}$ complexes.

TABLE 7: Bond Dissociation Enthalpies and Free Energies (kJ mol^{-1}) in the Gas Phase and Solution for the Ru(II)−G7 Bond in Bifunctional Complexes Including Larger Ligands

fragment	D_e	ΔH^{298}(g)	ΔG^{298}(g)	ΔH^{298}(aq)	ΔG^{298}(aq)	$\Delta\Delta G_{solv}$	G_{solv}(Ru)	G_{solv}
$[Ru(NH_3)_5]^{2+}$	362	317	256	105	45	−211	−820	−701
$[Ru(NH_3)_4Cl]^{+}$	234	226	169	102	45	−124	−297	−266
$[Ru(NH_3)_4(H_2O)]^{2+\,a}$	338	330	268	110	48	−221	−834	−706
$[Ru(NH_3)_4(H_2O)]^{2+\,b}$	353	345	283	126	64	−219	−834	−708
$[Ru(azpy)_2(H_2O)]^{2+}$	296	288	221	103	36	−185	−661	−569
$[Ru(bpy)_2\ (H_2O)]^{2+}$	286	281	210	114	42	−168	−627	−552

[a] With guanine−ammine hydrogen bond. [b] With guanine−water hydrogen bond.

TABLE 8: Energy Decomposition of the Ru−B Bonds in the C_s-Symmetric Complexes $[Ru(NH_3)_5B]^{2+}$

B	ΔE_{str}(B)	ΔE_{str}(Ru)	ΔE_{str}	ΔE_{Pauli}	ΔE_{elst}	ΔE_{orb}(a)	ΔE_{orb}(a)	ΔE_{orb}	ΔE_{Cs}	ΔE_{CsC1}
NH_3		8.07	8.10	292	−310	−143	−15.8	−159	168	0.0
Cl^-		19.4	19.4	433	−1111	−221	−43.1	−264	−924	0.0
H_2O	0.2	2.3	2.5	128	−151	−76.0	−9.9	−85.8	−107	1.7
Me_2S	2.88	15.4	18.3	420	−352	−221	−55.1	−276	−190	0.6
A1	8.36	15.5	23.9	363	−346	−180	−57.9	−238	−197	5.4
A3	7.34	11.6	18.9	386	−354	−187	−67.7	−255	−204	2.3
A7	3.64	14.1	17.8	382	−336	−183	−62.4	−245	−181	8.1
C	9.30	28.6	37.9	415	−443	−202	−68.8	−271	−261	0.3
G3	48.4	18.0	66.4	351	−293	−175	−60.0	−235	−109	0.0
G7	11.3	17.0	28.3	442	−499	−211	−84.7	−296	−324	2.4
MeIm	7.82	11.2	19.1	378	−399	−180	−52.7	−232	−235	2.5
$Me_2PO_4^-$	58.6	24.8	33.8	370	−1044	−222	−67.3	−289	−905	1.2

simple $[Ru(NH_3)_4Cl_2]$ species and the more active [*cis*-Ru(II)-$Cl_2(bpy)_2$] and [*cis*-Ru(II)$Cl_2(azpy)_2$] complexes with large polypyridyl and arylazopyridine ligands. In particular, due to the large size of the latter two complexes and the corresponding computational load, we considered only the binding of a guanine molecule (the most tightly bound nucleobase) to the aquated and reduced species which are expected to be actually present in vivo, $[Ru(NH_3)_4(H_2O)Cl]^+$ and $[Ru(NH_3)_4(H_2O)_2]^{2+}$, [*cis*-$Ru(H_2O)_2(bpy)_2]^{2+}$ and [*cis*-$Ru(H_2O)_2(azpy)_2]^{2+}$, optimizing their geometries and calculating the bond dissociation enthalpies and free energies of the Ru−guanine bond in $[Ru(NH_3)_4Cl$-$(G7)]^+$, $[Ru(NH_3)_4(H_2O)(G7)]^{2+}$, [*cis*-$Ru(bpy)_2(H_2O)(G7)]^{2+}$, and [*cis*-$Ru(azpy)_2(H_2O)(G7)]^{2+}$. The results are reported in Table 7 and allow evaluation of the effect of the presence of a second labile (chloro or aquo) coordination site and of more realistic polypyridyl and arylazopyridine ligands on the Ru−G7 bond dissociation energies. Table 7 shows that the presence of a chloro or an aquo ligand has a small effect on the dissociation enthalpy and free energy in solution of the Ru−G7 bond in $[Ru(NH_3)_5(G7)]^{2+}$. Going in more detail, the effect is negligible (ca. 5 kJ mol^{-1}) if the guanine maintains its hydrogen bond with one of the ammine ligands while it is significant (ca. 20 kJ mol^{-1}) if the guanine forms a stronger hydrogen bond with the aquo ligand. The optimized geometries of [*cis*-$Ru(bpy)_2(H_2O)(G7)]^{2+}$ and [*cis*-$Ru(azpy)_2(H_2O)(G7)]^{2+}$ show a hydrogen bond between the guanine carbonyl group and the aquo ligand, see Figure 2. However, Table 7 shows that replacement of the ammines by the polypyridyl or arylazopyridine ligands causes a small decrease, by 5−10 kJ mol^{-1}, of the Ru−G7 dissociation enthalpy and free energy in solution with respect to the corresponding $[Ru(NH_3)_4(H_2O)(G7)]^{2+}$ complex with the same guanine−aquo hydrogen bond.

3.4. Bond Analysis. We then analyzed the nature of the Ru−B bond in the $[Ru(NH_3)_5(B)]^{2+}$ complexes by employing the energy decomposition scheme developed by Ziegler and Rauk in C_s symmetry which allows separation of the orbital interaction contributions to the bond energy within the irreducible representations a′ and a″ corresponding to σ and π interactions. The results of the analysis are presented in Table 8, which reports all the contributions to the Ru−B bond dissociation energy and includes the Ru−B bond dissociation energy in C_s symmetry, ΔE_{Cs}, and the difference between the

bond dissociation energy of the asymmetric complex and the C_s-symmetrized one, $\Delta E_{CsC1} = \Delta E - \Delta E_{Cs}$.

The analysis indicates small strain energies for all the considered bases, below 10 kJ mol^{-1}, a larger value of 58.6 kcal mol^{-1} being observed for the dimethylphosphate anion. In all the considered complexes the electrostatic contribution has a larger stabilizing effect than the orbital interaction (150−1100 vs 100−300 kJ mol^{-1}), especially for the anionic dimethylphosphate base.

Particularly interesting is the analysis of the contribution from the a′ and a″ irreducible representation to the orbital interaction energy, which shows that σ interactions are always much more important than π interactions, respectively, 75−220 vs 10−85 kJ mol^{-1}. However, a significant contribution of the π interactions between the metal center and the ligand, ΔE_{orb}(a″), is observed for most of the considered bases, the largest one being observed for guanine with ca. 85 kJ mol^{-1}. Inspection of the gross atomic population of the frontier molecular orbitals of the two fragments shows that while for imidazole and all nucleobases the a″ contribution is mainly due to the π back-donation from the Ru(II) metal center to the π* ligand, for dimethylthioether and dimethylphosphate the a″ contribution is mainly due to π donation from the oxygen or sulfur lone pairs to the metal ion.

The difference between the bond dissociation energy of the asymmetric and C_s-symmetrized complex, ΔE_{CsC1}, is expected to arise from loss of part of the energy gain due to the hydrogen bond between an equatorial ammonia ligand and a carbonyl or an ammine group on the nucleobase. Indeed, in C_s symmetry the hydrogen-bond donor group cannot suitably orient toward one of the equatorial ammines to form a hydrogen bond, although it can form two weak hydrogen bonds with two adjacent ammines. Table 8 shows that the ΔE_{CsC1} values are significantly large only for the G7, A7, and A1 complexes whose optimized geometry reveals the presence of an hydrogen bond and, to a lesser extent, for MeIm. Note that the guanine, although forming a stronger hydrogen bond than adenine, shows a lower ΔE_{CsC1} value, probably since its carbonyl group can form a sufficiently strong hydrogen bond with two adjacent ammines in the C_s symmetry while the more directional amino group of adenine cannot.

3.5. Correlation between Bond Dissociation Energies and Proton Affinities or pK_a. The nature of the bond of a ligand L to a transition-metal ion is usually assumed to be strictly related to the proton affinity of the ligand L. Indeed, the proton affinity (PA) of L resembles the general preference of L to coordinate with cations and combines covalent and electrostatic interactions. Correlations of metal ligand dissociation energies with the proton affinities of the ligands have been reported for a series of bare and ligated cationic transition metal ions, and in some cases good correlations have been obtained.[44] To investigate whether there exists a direct correlation between the Ru−B gas-phase bond enthalpies and the proton affinities of the free bases B or between the Ru−B bond free energies in solution and the free bases pK_a values we calculated proton affinities and pK_a for all the considered bases, including all distinct basic sites for the nucleobases, at the same level of theory used for the ruthenium complexes (see Table S2). The accuracy of the calculated pK_a values is estimated from the comparison with the experimental values for the three considered nucleobases, MeIm, Me_2S, and $(MeO)_2PO_2^-$, which indicates good agreement, as shown by the plot of the experimental versus theoretical pK_a values with a R^2 value of 0.9735, see Figure S1. A remarkable correlation is observed between the Ru−B gas-phase bond enthalpies and the free base proton affinities for both Ru(II) and Ru(III) fragments (with correlation coefficients R^2 of 0.889 and 0.919, respectively), see Figure 3. This is not surprising, given that for all bases σ interactions are much more important than π interactions. On the other hand, no correlation is apparent between the Ru−B bond free energies in solution and the free bases pK_a values, the data being widely spread, see Figure 4, mainly due to the different effect of proton and metal binding to the base solvation energies. These results suggest that the proton affinities of the bases binding sites (but not their pK_a) can be used as a guideline to predict ruthenium affinities.

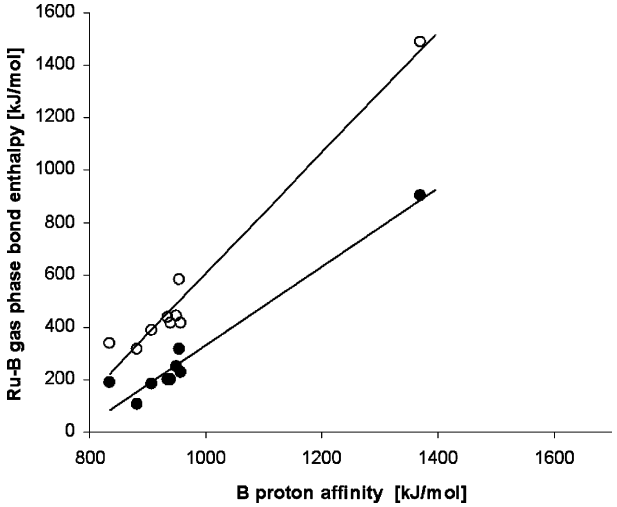

Figure 3. Ru−B bond dissociation enthalpies versus the proton affinities of the corresponding bases B: empty circles Ru(II) complexes; filled circles Ru(III) complexes.

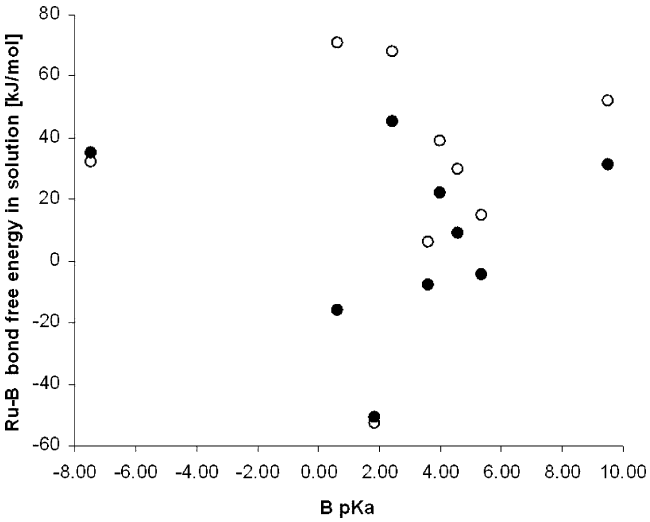

Figure 4. Ru−B bond dissociation free energies in solution versus the pK_a of the corresponding bases B: empty circles Ru(II) complexes; filled circles Ru(III) complexes.

4. Conclusions

The thermodynamics of the binding of the antitumor ammine, amine, and immine complexes of ruthenium(II) and ruthenium(III) to DNA and peptides was studied computationally using model complexes of the formula $[Ru(NH_3)_5B]^{z+}$, where B is an adenine, guanine, or cytosine nucleobase or a 4-methylimidazole, a dimethylthioether, or a dimethylphosphate anion, and $z = 2$ and 3. Calculated bond dissociation enthalpies and free energies allowed us to build a binding affinity order for the considered nucleic acid or protein binding sites both in the gas

phase and in solution. For Ru(II), the calculated binding order in solution is G(N7) > Me_2S > MeIm > A(N3) > C(N3) > A(N7) > A(N1) > $(MeO)_2PO_2^-$ > G(N3), indicating that the guanine N7 is the preferred site for ruthenium(II) binding, although the imidazole-containing histidyl residue or the sulfur-containing methionine and cysteine residues in proteins are a favorable binding site with binding free energies only 10−14 kJ mol^{-1} lower. The high bond energy for guanine N7 has also been attributed to formation of a strong hydrogen bond between guanine CO and one of the ammine ligands. These results indicate that ruthenium binds preferentially to guanine N7 but also to protein sites, in agreement with experimental evidence. A different binding order has been calculated for Ru(III)—$(MeO)_2PO_2^-$ > G(N7) > MeIm > A(N3) > Me_2S > C(N3) > A(N1) > A(N7) > G(N3)—indicating that the Ru(III)−phosphate is the strongest bond in aqueous solution, probably because of the stronger electrostatic interaction between the anionic phosphate and the tricationic Ru(III) fragment. This result is very different from that obtained for the Ru(II)−phosphate bond which is calculated to be unstable in solution and suggests that the Ru-(III) complexes in vivo could strongly bind to the phosphate anionic groups of the DNA backbone or also to other anionic groups on the proteins surfaces. Interestingly, this result is consistent with the experimentally observed low antitumor activity of the unreduced Ru(III) species and supports the activation by reduction mechanism.

The binding of some bifunctional complexes, $[Ru(NH_3)_4Cl_2]$, $[Ru(NH_3)_4(H_2O)_2]^{2+}$, [*cis*-$RuCl_2(bpy)_2$], and [*cis*-$RuCl_2(azpy)_2$], has also been considered to evaluate the effect of a second labile chloro or aquo ligand and of more realistic polypyridyl and arylazopyridine ligands. The results indicate that the presence of a chloro or aquo ligand has a negligible effect on the dissociation enthalpy and free energy in solution of the Ru guanine bond, while replacement of the ammines by the polypyridyl or arylazopyridine ligands causes a small decrease, by 5−10 kJ mol^{-1}, of the Ru guanine dissociation enthalpy and free energy in solution Finally, the results of the Ru−B bond energy analysis show that σ interactions are always much more important than π interactions, respectively, 80−220 vs 10−85 kJ mol^{-1}, although a significant contribution of the π interactions between the metal center and the ligand is observed for most of the considered bases.

Acknowledgment. The Italian Ministry for University and Research is acknowledged for financial support (contract 2006038520).

Supporting Information Available: Table with bond angles for the $[Ru(NH_3)_5(B)]^{z+}$ complexes, table with the proton affinities and pK_a values calculated for all the considered bases, and figure with the plot of the experimental versus theoretical pK_a values. This material is available free of charge via the Internet at http://pubs.acs.org.

References and Notes

(1) (a) Keppler, B. K. In *Progress in Clinical Biochemistry and Medicine;* Springer: Berlin, 1989; Vol. 10, p 41. (b) Clarke, M. J. In *Metal Complexes in Cancer Chemotherapy*; Keppler, B. K., Ed.; VCH: Weinheim, 1993; p 129. (c) Keppler, B. K.; Lipponer, K. G.; Stenzel, B.; Kratz, F. In *Metal Complexes in Cancer Chemotherapy*; Keppler, B. K., Ed.; VCH: Weinheim, 1993; pp 187−220. (d) Clarke, M. J.; Zu, F.; Frasca, D. R. *Chem. Rev.* **1999**, *99*, 2511−2533. (e) Clarke, M. J. *Coord. Chem. Rev.* **2002**, *232*, 69−93.

(2) (a) Ang, W. H.; Dyson, P. J. *Eur. J. Inorg. Chem.* **2006**, 4003−4018. (b) Brabec, V.; Novakova, O. *Drug Resistance Update* **2006**, *9*, 111−122.

(3) (a) Reedijk, J. *Proc. Natl. Acad. Sci. U.S.A.* **2003**, *100*, 3611. (b) Allardyce, C. S.; Dyson, P. J. *Platinum Met. Rev.* **2001**, *45*, 62−69.

(4) Frasca, D.; Ciampa, J.; Emerson, J.; Umans, R. S.; Clarke, M. J. *Met.-Based Drugs* **1996**, *3*, 197−209.

(5) (a) Van Vliet, P. M.; Toekimin, S. M. S.; Sarinten, M. S.; Haasnoot, J. G.; Reedijk, J.; Novakova, O.; Vrana, O.; Brabec, V. *Inorg. Chim. Acta* **1995**, *231*, 57−64. (b) Novakova, O.; Kasparkova, J.; Vrana, O.; Van Vliet, P. M.; Reedijk, J.; Brabec, V. *Biochemistry* **1995**, *34*, 12369−12378.

(6) Galanski, M.; Arion, V. B.; Jakupec, M. A.; Keppler, B. K. *Curr. Pharm. Des.* **2003**, *9*, 2078−2089.

(7) (a) Hartinger, C. G.; Zorbas-Seifried, S.; Jakupec, M. A.; Kynast, B.; Zorbas, H.; Keppler, B. K. *J. Inorg. Biochem.* **2006**, *100*, 891−904. (b) Jakupec, M. A.; Arion, V. B.; Kapitza, S.; Reisner, V.; Eichinger, A.; Pongratz, M.; Marian, B.; Graf, N.; Keyserlingk, V.; Keppler, B. K. *Int. J. Clin. Pharmacol. Ther.* **2005**, *43*, 595−596.

(8) Kapitza, S.; Pongratz, M.; Jacupec, M. A.; Heffeter, P.; Berger, W.; Lackinger, L.; Keppler, B. K.; Marian, B. *J. Cancer Res. Clin. Oncol.* **2005**, *131*, 101−110.

(9) (a) Velders, A. H.; Kooijman, H.; Spek, A. L.; Haasnoot, J. G.; de Vos, D.; Reedijk, J. *Inorg. Chem.* **2000**, *39*, 2966−2967. (b) Hotze, A. C. G.; Velders, A. H.; Ugozzoli, F.; Biagini-Cingi, M.; Manotti-Lanfredi, A. M.; Haasnoot, J. C.; Reedijk, J. *Inorg. Chem.* **2000**, *39*, 3838−3844. (c) Hotze, A. C. G.; Caspers, S. E.; de Vos, D.; Kooijman, H.; Spek, A. L.; Flamini, A.; Babac, M.; Sava, G.; Haasnoot, J. G.; Reedijk, J. *J. Biol. Inorg. Chem.* **2004**, *9*, 354−364.

(10) (a) Alessio, E.; Mestroni, G.; Nardin, G.; Attia, W. M.; Calligaris, M.; Sava, G.; Zorzet, S. *Inorg. Chem.* **1988**, *27*, 4099−4106. (b) Sava, G.; Pacor, S.; Zorzet, S.; Alessio, E.; Mestroni, G. *Pharmacol. Res.* **1989**, *21*, 617−628.

(11) Sava, G.; Pacor, S.; Mestroni, G.; Alessio, E. *Anti-Cancer Drugs* **1992**, *3*, 25.

(12) (a) Sava, G.; Gagliardi, R.; Bergamo, A.; Alessio, E.; Mestroni, G. *Anticancer Res.* **1999**, *19*, 969−972. (b) Alessio, E.; Mestroni, G.; Bergamo, A.; Sava, G. *Curr. Top. Med. Chem.* **2004**, *4*, 1525−1535. (c) Rademaker-Lakhai, J. M.; Van Den Bongard, D.; Pluim, D.; Beijnen, J. H.; Schellens, J. H. M. *Clin. Cancer Res.* **2004**, *10*, 3717−3727.

(13) Gopal, Y. N. V.; Konuru, N.; Kondapi, A. K. *Arch. Biochem. Biophys.* **2002**, *401*, 53−62.

(14) (a) Yan, Y. K.; Melchart, M.; Habtemariam, A.; Sadler, P. J. *Chem. Commun.* **2005**, 4764−4776. (b) Peacock, A. F. A.; Habtemariam, A.; Fernandez, R.; Walland, V.; Fabbiani, F. P. A.; Parsons, S.; Aird, R. E.; Jodrell, D. I.; Sadler, P. J. *J. Am. Chem. Soc.* **2006**, *128*, 1739−1748.

(15) (a) Clarke, M. J.; Jansen, B.; Marx, K. A.; Kruger, R. *Inorg. Chim. Acta* **1986**, *124*, 13−28. (b) McNamara, M.; Clarke, M. J. *Inorg. Chim. Acta* **1992**, *195*, 175−185.

(16) (a) Messori, L.; Vilchez, F. G.; Vilaplana, R.; Piccioli, F.; Alessio, E.; Keppler, B. K. *Met.-Based Drugs* **2000**, *7*, 335. (b) Messori, L.; Orioli, P.; Vullo, D.; Alessio, E.; Iengo, E. *Eur. J. Biochem.* **2000**, *267*, 1206.

(17) (a) Messori, L.; Kratz, F.; Alessio, E. *Met.-Based Drugs* **1996**, *3*, 1. (b) Smith, C. A.; Sutherland-Smith, A. J.; Keppler, B. K.; Kratz, F.; Baker, E. N. *J. Biol. Inorg. Chem.* **1996**, *1*, 424. (c) Frasca, D. R.; Gehrig, L. E.; Clarke, M. J. *J. Inorg. Biochem.* **2001**, *83*, 139. (d) Pongratz, M.; Schluga, P.; Jakupec, M. A.; Arion, V. B.; Hartinger, C. G.; Allmaier, G.; Keppler, B. K. *J. Anal. At. Spektrom.* **2004**, *19*, 46−51.

(18) (a) Frasca, D.; Clarke, M. J. *J. Am. Chem. Soc.* **1999**, *121*, 8523. (b) Zhao, M.; Clarke, M. J. *J. Biol. Inorg. Chem.* **1999**, *4*, 318−340.

(19) (a) Kuehn, C. G.; Taube, H. *J. Am. Chem. Soc.* **1976**, *98*, 689. Fruhauf, S.; Zeller, W. J. *Cancer Res.* **1991**, *51*, 2943−2948. (b) Gallori, E.; Vettori, C.; Alessio, E.; Vilchez, F. G.; Vilaplana, R.; Orioli, P.; Casini, A.; Messori, L. *Arch. Biochem. Biophys.* **2000**, *376*, 156−162.

(20) Cotton, F. A.; Wilkinson, G. *Advanced Inorganic Chemistry*; John Wiley & Sons: New York, 1988.

(21) Jamieson, E. R.; Lippard, S. J. *Chem. Rev.* **1999**, *99*, 2467.

(22) (a) Isied, S.; Taube, H. *Inorg. Chem.* **1976**, *15*, 3070. (b) Novakova, O.; Hofr, C.; Brabec, V. *Biochem. Pharmacol.* **2000**, *60*, 1761−1771.

(23) Malina, J.; Novakova, O.; Keppler, B. K.; Alessio, E.; Brabec, V. *J. Biol. Inorg. Chem.* **2001**, *6*, 435−445.

(24) Gopal, Y. N. V.; Jayaraju, D.; Kondapi, A. K. *Biochemistry* **1999**, *38*, 4382−4388.

(25) (a) Frasca, D. R.; Clarke, M. J. *J. Am. Chem. Soc.* **1999**, *121*, 8523. (b) Jakupec, M. A.; Reisner, E.; Eichinger, A.; Pongratz, M.; Arion, V. B.; Galanski, M.; Hartinger, C. G.; Keppler, B. K. *J. Med. Chem.* **2005**, *48*, 2831.

(26) Okunieff, P.; Dunphy, E. P.; Vaupel, P. *Adv. Exp. Med. Biol.* **1994**, *345*, 485.

(27) Miklavcic, D.; Sersa, G.; Novakovic, S. *J. Bioelect.* **1990**, *9*, 133.

(28) Marchant, J. A.; Matsubara, T.; Ford, P. C. *Inorg. Chem.* **1977**, *16*, 2160.

(29) Clarke, M. J.; Bitler, S.; Rennert, D.; Buchbinder, M.; Kelman, A. D. *J. Inorg. Biochem.* **1980**, *12*, 79−87.

(30) (a) Clarke, M. J. *Inorg. Chem.* **1977**, *6*, 738. (b) Clarke, M. J. *J. Am. Chem. Soc.* **1978**, *100*, 5068. (c) Kastner, M. E.; Coffey, K. F.; Clarke, M. J.; Edmonds, S. E.; Eriks, K. *J. Am. Chem. Soc.* **1981**, *103*, 5747. (d)

Bailey, V. M.; Clarke, M. J. *Inorg. Chem.* **1997**, *36*, *1611*. (e) LaChance-Galang, K.; Zhao, M.; Clarke, M. J. *Inorg. Chem.* **1996**, *35*, 6021. (f) Bailey, V. M.; LaChance-Galang, K. J.; Doan, P. E.; Clarke, M. J. *Inorg. Chem.* **1997**, *36*, 1873.

(31) (a) Hotze, A. C. G.; van der Geer, E. P. L.; Caspers, S. E.; Kooijman, H.; Spek, A. L.; Haasnoot, J. G.; Reedijk, J. *Inorg. Chem.* **2004**, *43*, 4935−4943. (b) Zobi, F.; Hohl, M.; Zimmermann, I.; Alberto, R. *Inorg. Chem.* **2004**, *43*, 2771−2772. (c) Egger, A.; Arion, V. B.; Reisner, E.; Cebrián-Losantos, B.; Shova, S.; Trettenhahn, G.; Kepler, B. K. *Inorg. Chem.* **2005**, *44*, 122−132.

(32) Cini, R.; Tommasi, G.; Defazio, S.; Corsini, M.; Zanello, P.; Messori, L.; Marcon, G.: Piccioli, F.; Orioli, P. *Inorg. Chem.* **2003**, *42*, 8038−8052.

(33) (a) Chen, J. C.; Li, J.; Qian, L.; Zheng, K. C. *J. Mol. Struct.* (*THEOCHEM*) **2005**, *728*, 93−101. (b) Scolaro, C.; Geldbach, T. J.; Rochat, S.; Dorcier, A.; Gossens, C.; Bergamo, A.; Cocchietto, M.; Tavernelli, I.; Sava, G.; Rothlisberger, U.; Dyson, P. J. *Organometallics* **2006**, *25*, 756−765.

(34) (a) Boerrigter, P. M.; te Velde, G.; Baerends, E. J. *Int. J. Quantum Chem.* **1988**, *33*, 87. (b) Te Velde, G.; Baerends, E. J. *J. Comput. Phys.* **1992**, *99*, 84.

(35) Vosko, S. H.; Wilk, L.; Nusair, M. *Can. J. Phys.* **1980**, *58*, 1200.

(36) Becke, A. D. *Phys. Rev.* **1988**, *A38*, 2398.

(37) Perdew, J. P. *Phys. Rev.* **1986**, *B33*, 8822.

(38) (a) Ziegler, T.; Tshinke, V.; Baerends, E. J.; Snijders, J. G.; Ravenek, W. *J. Phys. Chem.* **1989**, *93*, 3050. (b) Boerrigter, P. M. Spectroscopy and Bonding of Heavy Element Compounds. Ph.D. Thesis, Vrije University, 1987. Li, J.; Schreckenbach, G.; Ziegler, T. *J. Am. Chem. Soc.* **1995**, *117*, 486 and references therein.

(39) (a) Klamt, A.; Schürmann, G. *J. Chem. Soc., Perkin Trans. 2* **1993**, 799. (b) Pye, C. C.; Ziegler, T. *Theor. Chem. Acc.* **1999**, *101*, 396.

(40) (a) Ziegler, T.; Rauk, A. *Theor. Chim. Acta* **1977**, *46*, 1. (b) Ziegler, T. *NATO ASI* **1986**, *C176*, 189.

(41) Baik, M.-Y.; Friesner, R. A.; Lippard, S. J. *J. Am. Chem. Soc.* **2003**, *125*, 14082−14092.

(42) Burda, J. V.; Šponer, J.; Leszczynski, J. *J. Biol. Inorg. Chem.* **2000**, *5*, 178−188.,

(43) Burda, J. V.; Leszczynski, J. *Inorg. Chem.* **2003**, *42*, 7162−7172.

(44) (a) Martinho-Simoñes, J. A.; Beauchamp, J. L. *Chem. Rev.* **1990**, *90*, 629. (b) Operti, L.; Tews, E. C.; Freiser, B. S. *J. Am. Chem. Soc.* **1988**, *110*, 3847 and references therein.